

More Rigid Macrocyclic Ligands That Show Metal Ion Size-Based Selectivity. A Crystallographic, Molecular Mechanics, and Formation Constant Study of the Complexes of Bridged Cyclen

Robert D. Hancock,*† Susan M. Dobson,† Ann Evers,† Peter W. Wade,†
M. Patrick Ngwenya,† Jan C. A. Boeyens,† and Kevin P. Wainwright‡

Contribution from the Departments of Chemistry, University of the Witwatersrand, Johannesburg, South Africa, and The Flinders University of South Australia, Bedford Park, South Australia.
Received June 19, 1987

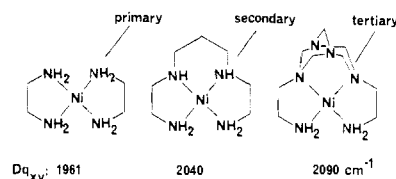
Abstract: The formation constants of the bridged cyclen (1,4,7,10-tetraazabicyclo[8.2.2]tetradecane) ligand are reported with Cu(II), Ni(II), Zn(II), Cd(II), and Pb(II). The bridge on the ligand leads to enhanced metal ion selectivity based on the match between the size of the metal ion and that of the cavity in the ligand. The macrocyclic effect, i.e. the difference in $\log K_1$ for the complexes of the bridged cyclen and its open-chain analogue at 9.6 log units, is the largest recorded to date. The crystal structure of the perchlorate complex of low-spin Ni(II) with the bridged cyclen is reported. The yellow crystals of $[\text{Ni}(\text{C}_{10}\text{H}_{22}\text{N}_4)](\text{ClO}_4)_2$ crystallized in the orthorhombic space group $P2_12_12_1$ with $a = 9.176$ (6), $b = 12.981$ (2), and $c = 14.419$ (2) Å. The value of Z was 4, V was 1717.6 Å³, d_m was 1.77 g·cm⁻³, and d_c was 1.76 g·cm⁻³. The final conventional R factor was 0.052. The Ni–N bond lengths averaged 1.867 (4) Å, which is unusually short for low-spin Ni(II) with a polyamine ligand, suggesting compression of the metal ion by the ligand. A molecular mechanics analysis of the structures of several complexes of low-spin Ni^{II} with polyamine ligands was carried out. Force field parameters appropriate to low-spin Ni^{II} are reported. The MM calculations on the bridged cyclen complex of low-spin Ni^{II} confirm that the Ni–N bond lengths are compressed, by about 0.05 Å. The information on the complexing properties of bridged cyclen gained from the formation constants, the crystal structure, and the MM calculations is used to discuss the unusual selectivity patterns and ligand field strength of the ligand.

An important idea in macrocyclic chemistry is that of the relatively rigid cavity in the center of the ligand, which produces enhanced complex stability when there is a match between the size of the cavity and that of the metal ion being complexed.^{1,2} In this paper such selectivity will be referred to as size-match selectivity. A second idea, which appears to be widely accepted, is that the macrocycle is sufficiently rigid to compress a too-large metal ion. This idea has been postulated³ to account for the very high ligand field (LF) strength observed in the complexes of some N-donor macrocycles with metal ions such as Ni(II) and Co(III). Recent evidence has suggested that these ideas may need some modification. For the series of N-donor macrocycles (see Figure 1 for key to ligand abbreviations) 12-aneN₄ to 15-aneN₄, it has been shown^{4,5} that the variation of the formation constants of a variety of metal ions along the series is almost exactly opposite to what would be expected if size-match selectivity were controlling ligand selectivity for different metal ions.

The hole sizes of the tetraaza macrocycles were estimated by molecular mechanics (MM) calculations.^{3,6} In all cases the MM calculations were carried out on the *trans*-III conformers of the complexes (see Figure 2) and showed a steady increase in hole size from 12-aneN₄ through 16-aneN₄. However, other conformers of the complexes exist, and in the *trans*-I (see Figure 2) and folded *cis*-V conformers in particular, the metal ion is coordinated in an out-of-plane mode. The out-of-plane mode of coordination, as shown by MM analysis,⁷ leads to loss of size-match selectivity. What is clearly needed are ligands that are more rigid and constrain the metal ion to coordinate lying in the plane of the donor atoms.

The Ni–N bond lengths in complexes such as $[\text{Ni}(\text{en})_2]^{2+}$ at 1.92 Å⁸ are very similar to those found in tetraaza macrocyclic complexes of low-spin Ni(II). Fabbri⁹ observed that the high LF in the tetraaza macrocyclic complexes occurred where the fit into the macrocyclic cavity was exact, which did not accord with the compression hypothesis. It was subsequently proposed^{6,10} that the high LF strengths were due to the greater donor strength of the nitrogens along the series primary, secondary, tertiary as seen

Chart I



in a series such as that shown in Chart I. It must be emphasized that in many cases the greater donor strength of higher order nitrogens is masked by steric effects. Thus, the low LF strength in $[\text{Ni}(\text{TMC})]^{2+}$ is reasonably attributed¹⁰ to the stretching of the Ni–N bonds out to the very long values observed, by van der Waals repulsions between the methyl groups.

The ligand (1,4-C₂)-12-aneN₄ (Figure 1) is of particular interest. As reported in a recent communication,¹¹ the LF strength of $[\text{Ni}((1,4\text{-C}_2)\text{-12-aneN}_4)]^{2+}$ with $Dq_{xy} = 2180$ cm⁻¹ is by a wide margin much higher than that for any other complex of low-spin Ni(II) with saturated nitrogen donors. The ligand has two tertiary and two secondary nitrogens, which may contribute to the high LF strength. However, models show that there is very little space in the cavity of (1,4-C₂)-12-aneN₄, and this may be a genuine example of a compression-induced increase in LF strength.

(1) Pedersen, C. J. *J. Am. Chem. Soc.* **1967**, *89*, 7017–7036.

(2) Lehn, J. M. *Acc. Chem. Res.* **1978**, *11*, 49–57.

(3) Busch, D. H. *Acc. Chem. Res.* **1978**, *11*, 393–400.

(4) Thöm, V. J.; Hosken, G. D.; Hancock, R. D. *Inorg. Chem.* **1985**, *24*, 3378–3381.

(5) Thöm, V. J.; Hancock, R. D. *J. Chem. Soc., Dalton Trans.* **1985**, 1877–1880.

(6) Hancock, R. D.; McDougall, G. J. *J. Am. Chem. Soc.* **1980**, *102*, 6551–6553.

(7) Thöm, V. J.; Fox, C. C.; Boeyens, J. C. A.; Hancock, R. D. *J. Am. Chem. Soc.* **1984**, *106*, 5947–5955.

(8) Stomberg, R. *Acta Chem. Scand.* **1969**, *23*, 3498–3512.

(9) Fabbri, L. *J. Chem. Soc., Dalton Trans.* **1979**, 1857–1861.

(10) Thöm, V. J.; McDougall, G. J.; Boeyens, J. C. A.; Hancock, R. D. *J. Am. Chem. Soc.* **1984**, *106*, 3198–3207.

(11) Wainwright, K. P.; Ramasubba, A. *J. Chem. Soc., Chem. Commun.* **1982**, 277.

*University of Witwatersrand.

†The Flinders University of South Australia.

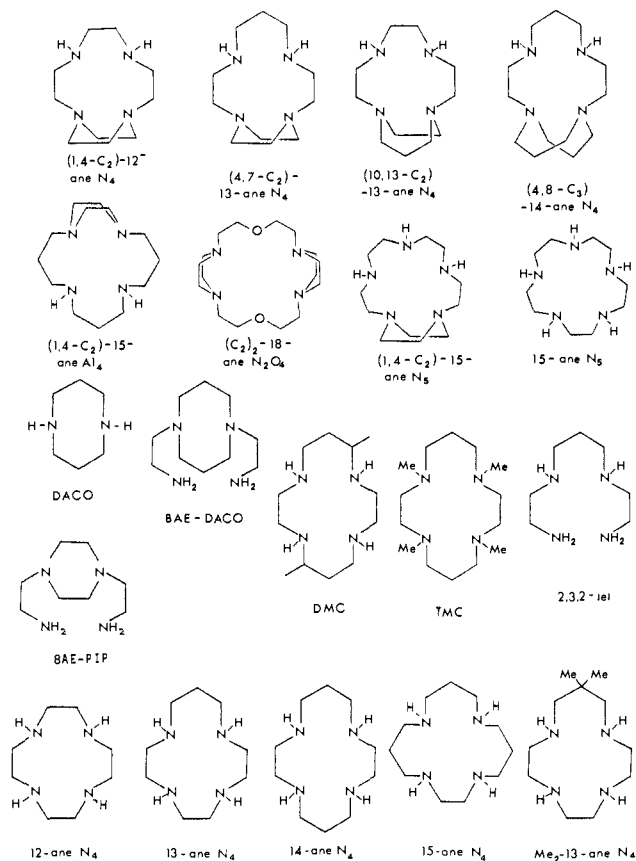


Figure 1. Ligands discussed in this paper.

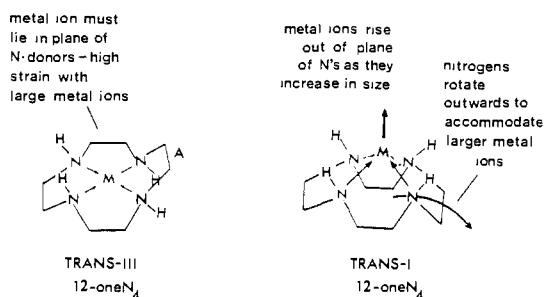


Figure 2. *trans*-I and *trans*-III conformers of 12-ane N_4 , showing how the *trans*-III conformer shows preferences for metal ions that fit into its macrocyclic cavity, while the *trans*-I conformer is able to accommodate a wide variety of metal ion sizes.

Further, the rigidity of the ligand shown by models suggests that out-of-plane coordination of metal ions will be highly strained. The ligand (1,4- C_2)-12-ane N_4 may thus be able to show genuine size selectivity. In this paper is thus reported a formation constant study on the complexes of (1,4- C_2)-12-ane N_4 with Ni^{2+} , Cu^{2+} , Zn^{2+} , Cd^{2+} , and Pb^{2+} , which provide a range of metal ion sizes from the very small low-spin $Ni(II)$ ion to the very large $Pb(II)$ ion. Also reported is a crystallographic study of $[Ni(1,4-C_2)-12-aneN_4](ClO_4)_2$ aimed at investigating the possibility of Ni-N bond length compression.

In order to investigate the question of bond length compression more thoroughly, a MM analysis of the structure of low-spin $Ni(II)$ complexes with nitrogen donor ligands was carried out. Parameters for low-spin $Ni(II)$ were developed with structures that display a wide range of Ni-N bond lengths (1.85–1.99 Å) and N-Ni-N bond angles (77.3–95.0°) to ensure their general applicability. Structures of low-spin $Ni(II)$ used in developing the parameters were $[Ni(en)_2]^{2+}$,⁸ $[Ni(TMC)]^{2+}$,¹² $[Ni(DMC)]^{2+}$,¹³ and $[Ni((1,4-C_2)-12-aneN_4)]^{2+}$ (this work). Also

examined were $[Ni(DACO)_2]^{2+}$ ¹⁴ and $[Ni(Me_2-13-aneN_4)]^{2+}$,¹⁵ which unfortunately had high R factors reported for the crystallographic analysis but which had interesting structural features. Much less weight was given to the latter two structures in fitting the parameters.

In previous work^{4,5} it has been shown that the selectivity patterns of the tetraaza macrocycles are controlled more by chelate ring size than by macrocyclic ring size. Thus, although the macrocyclic ring size increases steadily^{3,6} along the series 12-ane N_4 through 15-ane N_4 , the formation constants for a large metal ion such as Pb^{2+} decrease steadily with increasing macrocyclic ring size. This pattern resembles very strongly the changes in complex stability, which occur in nonmacrocyclic ligand pairs where the size of the *chelate* ring is increased; i.e., there is a strong decrease in complex stability for the complexes of larger metal ions. The effect of the doubly bridged chelate ring present in ligands such as (1,4- C_2)-12-ane N_4 on complex stability should thus also be of considerable interest.

Experimental Section

Materials. The ligand (1,4- C_2)-12-ane N_4 was synthesized as described previously,¹¹ as was also the complex $[Ni((1,4-C_2)-12-aneN_4)](ClO_4)_2$. Nitrate salts of metal ions used in the potentiometric study were obtained as AR salts, and stock solutions of these were standardized by routine methods.

Potentiometry. Potentiometric measurements were made with a cell thermostated to 25 °C, a Radiometer PHM84 pH meter, and a Radiometer G202B glass electrode with a Ag/AgCl reference electrode, under an atmosphere of nitrogen. The determination of the protonation constants of the ligand were straightforward, but equilibration times of the ligand with the metal ion were somewhat long to allow use of conventional glass-electrode potentiometry. The formation constants were thus determined in out-of-cell titrations as described by ourselves⁵ and other workers.^{16,17} Approximately 12 solutions were prepared for each metal ion, each solution corresponding to a single point in a potentiometric titration, and these solutions were allowed to equilibrate for a few weeks in a water bath. The pH of these solutions was measured several times, and attainment of a constant pH reading was taken as an indication that equilibrium had been achieved. The potentiometric data were processed with the program MINQUAD¹⁸ and also EQUILIBRIA.¹⁹ It was found that a simple model involving no protonated (MLH) complexes fitted the data adequately, only ML complexes being present. No hydroxy complexes were detected (MLOH), although the pH range for titrations did not extend above a value of 7, and it is quite possible that hydroxy complexes would exist in the higher pH range. The protonation constants and equilibrium constants so determined are seen in Table I.

Crystallography. Yellow crystals of $[Ni((1,4-C_2)-12-aneN_4)](ClO_4)_2$ were recrystallized from acetonitrile to yield rod-shaped crystals suitable for crystallography. The density determination was carried out by flotation in a mixture of 1,2-dibromoethane and 1,2-dichloroethane. The cell dimensions were obtained from a least-squares refinement of 25 reflections (θ range from 16° to 20°). Data collection was carried out at room temperature on an Enraf-Nonius CAD4 diffractometer with graphite-monochromatized Mo $K\alpha$ radiation using an ω - 2θ scan mode. Three standard reflections were measured at regular intervals and showed less than 2% variation. Corrections for L_p and absorption were applied to the data. Absorption corrections were done by the method of Philips et al.,²⁰ with transmission factors from 0.9895 to 0.9012. The structure was solved by Patterson and difference Fourier methods. The perchlorate anions were disordered and were refined as disordered pairs with common chlorine atoms. Hydrogen atoms were placed in calculated positions and together with the oxygen atoms were refined isotropically, the remainder of the atoms being refined anisotropically. Full-matrix least-squares refinement with unit weights converged to $R = 0.052$ with shifts of less than 0.6σ . Residual electron density was between +0.53 and $-0.61 e \text{ \AA}^{-3}$. The data collection and processing parameters are summarized in Table

(13) Krajewski, Z.; Urbanczyk-Lipkowska, Z.; Gluzinski, P. *Bull. Acad. Pol. Sci., Ser. Sci. Chim.* **1977**, *25*, 853.

(14) Boeyens, J. C. A.; Fox, C. C. S. *Afr. J. Chem.* **1984**, *37*, 1–4.

(15) Waters, J. M.; Wittle, K. R. *J. Inorg. Nucl. Chem.* **1972**, *34*, 155–161.

(16) Zompa, L. J. *Inorg. Chem.* **1978**, *17*, 2531–2536.

(17) Micheloni, M.; Paoletti, P.; Sabatini, A. *J. Chem. Soc., Dalton Trans.* **1983**, 1189–1191.

(18) Sabatini, A.; Vacca, A.; Gans, P. *Talanta* **1974**, *21*, 53–59.

(19) Wade, P. W.; Hancock, R. D., to be submitted for publication.

(20) North, A. C. T.; Phillips, D. C.; Scott-Mathews, F. *Acta Crystallogr., Sect. A: Cryst. Phys., Diffr., Theor. Gen. Crystallogr.* **1968**, *A24*, 351–359.

(12) Hambley, T. W. *J. Chem. Soc., Dalton Trans.* **1986**, 565–569.

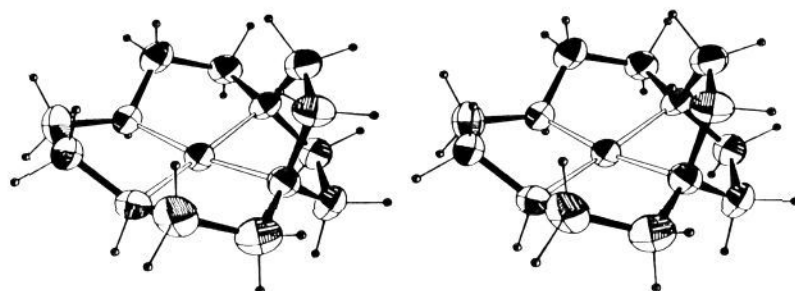
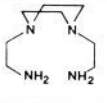
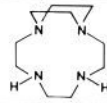
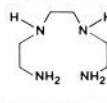
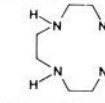


Figure 3. Stereoview of the complex cation $[\text{Ni}((1,4\text{-C}_2)\text{-12-aneN}_4)]^{2+}$.

Table I. Protonation and Formation Constants of Bridged and Nonbridged Tetraaza Macrocyclic Ligands and of Their Open-Chain Analogues^a

				log $K(\text{MAC})^e$			log $K(\text{MAC})^e$	r^{+f}	$\Delta \log K^g$
H^+	$\text{p}K_1^b$	9.64 ^c	10.90 (5) ^d		9.74 ^h	10.6 ^h			
	$\text{p}K_2$	8.98	10.31 (5)		9.07	9.6			
	$\text{p}K_3$	5.14	6.50 (2)		6.56	~1.2			
	$\text{p}K_4$		3.18 (2)		3.25				
$\log K_1$	$\text{Ni}^{2+}(S=0)^i$	4.68	14.3 (1) ^j	9.6	12.1 ⁱ	14.4 ^j	2.3	0.49 ^j	-0.1
	Cu^{2+}	11.91	21.50 (5)	9.6	20.1	23.3	3.2	0.57	-1.8
	Zn^{2+}	5.81	10.95 (6)	5.1	12.0	16.2	4.2	0.74	-5.2
	Cd^{2+}	4.51	10.07 (6)	5.6	10.6	14.3	3.7	0.95	-4.2
	Pb^{2+}	~7.1	11.71 (7)	~4.7	10.4	15.9	5.5	1.18	-4.2

^aThe ligands are from left to right: BAE-PIP, (1,4-C₂)-12-aneN₄, trien, and 12-aneN₄. ^bThe protonation constants refer to the following equilibria: $\text{p}K_1, \text{L} + \text{H}^+ \rightleftharpoons \text{LH}^+$; $\text{p}K_2, \text{LH}^+ + \text{H}^+ \rightleftharpoons \text{LH}_2^{2+}$; $\text{p}K_3, \text{LH}_2^{2+} + \text{H}^+ \rightleftharpoons \text{LH}_3^{3+}$; $\text{p}K_4, \text{LH}_3^{3+} + \text{H}^+ \rightleftharpoons \text{LH}_4^{4+}$. L is the ligand in each case. ^cReference 27 (25 °C, 0.1 M NaNO₃). ^dThis work (25 °C, 0.1 M NaNO₃). Numbers in parentheses indicate standard deviations in last significant figure reported. ^elog $K(\text{MAC})$ is log K_1 for the macrocyclic complex minus log K_1 for its open-chain analogue. ^fThe ionic radii of each metal ion (Å) from ref 28. ^gThe value of $\Delta \log K$ is log K_1 for the complex of the bridged macrocycle (1,4-C₂)-12-aneN₄ minus log K_1 for the complexes of its nonbridged analogue 12-aneN₄. ^hFrom ref 29. ⁱThese refer to low-spin ($S=0$) Ni^{II}. Since high-spin Ni^{II} is much larger than low-spin Ni^{II}, we would expect the concentration of the high-spin Ni^{II} complex of (1,4-C₂)-12-aneN₄ to be very small, as is supported experimentally.¹¹ Thus, comparisons can only be made with $S=0$ complexes of the other ligands in the table. It is not known at this stage what proportion of low-spin Ni^{II} is present in the complex with BAE-PIP.

Table II. Summary of Data Collection and Processing Parameters for $[\text{Ni}((1,4\text{-C}_2)\text{-12-aneN}_4)](\text{ClO}_4)_2$

cryst dimens, mm	0.12 × 0.18 × 0.46
cryst syst	orthorhombic
space gp	$P2_12_1$
cell dimens	
<i>a</i> , Å	9.176 (6)
<i>b</i> , Å	12.981 (2)
<i>c</i> , Å	14.419 (2)
<i>V</i> , Å ³	1717.6
<i>d_m</i> , g·cm ⁻³	1.77 (1)
<i>d_c</i> , g·cm ⁻³	1.76
<i>Z</i>	4
$\mu(\text{Mo K}\alpha)$	14.03
<i>F</i> (000)	944
data colln range	$3^\circ \leq \theta \leq 30^\circ$
scan width, deg	0.6 + 0.35 tan θ
scan speed, deg·min ⁻¹	1.0–4.1
range of <i>hkl</i>	0 → 12, 0 ≥ 18, 0 → 20
total no. of data coll'd	2848
no. of unique data after merging	2573
<i>R_{int}</i>	0.018
data with $I > 1.5\sigma(I)$	2056
total no. of variables	213
<i>R</i>	0.052

II. Fractional atomic coordinates are seen in Table III, and bond lengths and angles for the complex cation are seen in Table IV. Anisotropic temperature factors for non-hydrogen atoms, fractional coordinates for hydrogen atoms, and calculated and observed structure factors are available as supplementary material. The program SHELX-76²¹ was used for crystallographic calculations. The structure of the complex cation is shown in stereoview in Figure 3, and the numbering scheme is seen in Figure 4.

Table III. Fractional Coordinates ($\times 10^4$) and Equivalent Isotropic Temperature Factors ($\text{Å}^2, \times 10^3; \times 10^4$ for Ni and Cl) for Cation and Chlorine Atoms of $[\text{Ni}(\text{C}_{10}\text{H}_{22}\text{N}_4)(\text{ClO}_4)_2]$

	<i>x/a</i>	<i>y/b</i>	<i>z/c</i>	<i>U</i> (eq) ^a
Ni	2669 (1)	868 (1)	1365 (1)	317 (2)
N(1)	3799 (7)	1816 (5)	2001 (5)	38 (1)
N(2)	4263 (7)	11 (6)	1119 (5)	39 (1)
N(3)	1337 (7)	-97 (5)	893 (5)	38 (1)
N(4)	1195 (7)	1675 (6)	1882 (5)	38 (1)
C(1)	5325 (9)	1507 (8)	1875 (7)	50 (2)
C(2)	5389 (9)	345 (8)	1790 (7)	50 (2)
C(3)	3649 (9)	-1041 (6)	1233 (6)	48 (2)
C(4)	2111 (11)	-1107 (6)	817 (6)	56 (2)
C(5)	88 (8)	31 (6)	1546 (6)	43 (2)
C(6)	-217 (8)	1182 (7)	1628 (7)	45 (2)
C(7)	1571 (9)	2722 (6)	1519 (8)	45 (2)
C(8)	3266 (9)	2825 (7)	1630 (6)	44 (2)
C(9)	3256 (9)	1714 (8)	2977 (6)	45 (2)
C(10)	1527 (10)	1669 (9)	2897 (7)	51 (2)
Cl(1)	2788 (2)	1267 (2)	-1076 (1)	432 (4)
Cl(2)	-2572 (3)	733 (2)	4441 (2)	630 (5)

$$^a U(\text{eq}) = \frac{1}{3} \sum_i \sum_j U_{ij} a_i^* a_j^* (a_i a_j)$$

Molecular Mechanics Calculations. The program used for the MM calculations was MOLBLD-3 due to Boyd.²² The force field parameters appropriate to the organic part of the complex were as described previously.²⁴ A trial set of force field parameters to involve the low-spin Ni^{II} were used to calculate the structures of the four complexes listed in Table VI. The structure of the $[\text{Ni}((1,4\text{-C}_2)\text{-12-aneN}_4)]^{2+}$ cation was predicted before the structure determination was carried out, by the trial force field. This structure is compared in Figure 4 with that actually determined

(22) Boyd, R. H.; Breitling, S. M.; Mansfield, M. *Am. Inst. Chem. Eng. J.* **1973**, *19*, 1016–1024.

(23) Johnson, C. K. ORTEP Report No. ORNL-3794; Oak Ridge National Laboratory: Oak Ridge, TN, 1965.

(24) McDougall, G. J.; Hancock, R. D.; Boeyens, J. C. A. *J. Chem. Soc., Dalton Trans.* **1978**, 1438–1444.

(21) Sheldrick, G. M. In *Computing in Crystallography*; Schenk, H., Olthof-Hazelkamp, R., Van Koningsveld, H., Bassi, G. C., Eds.; Delft University: Delft, Holland, 1978.

Table IV. Important Bond Lengths and Bond Angles in the Complex Cation of $[\text{Ni}((1,4\text{-C}_2)\text{-12-aneN}_4)](\text{ClO}_4)_2^a$

Lengths, Å			
Ni-N(1)	1.852 (7)	Ni-N(2)	1.872 (7)
Ni-N(3)	1.877 (7)	Ni-N(4)	1.866 (7)
N(1)-C(1)	1.47 (1)	N(1)-C(8)	1.50 (1)
N(1)-C(9)	1.50 (1)	N(2)-C(2)	1.48 (1)
N(2)-C(3)	1.49 (1)	N(3)-C(4)	1.50 (1)
N(3)-C(5)	1.49 (1)	N(4)-C(6)	1.49 (1)
N(4)-C(7)	1.50 (1)	N(4)-C(10)	1.49 (1)
C(1)-C(2)	1.51 (1)	C(3)-C(4)	1.54 (1)
C(5)-C(6)	1.53 (1)	C(7)-C(8)	1.57 (1)
C(9)-C(10)	1.59 (1)		
Angles, deg			
N(1)-Ni-N(2)	92.9 (3)	N(1)-Ni-N(3)	170.7 (3)
N(2)-Ni-N(3)	92.5 (3)	N(1)-Ni-N(4)	80.5 (3)
N(2)-Ni-N(4)	167.3 (3)	N(3)-Ni-N(4)	92.7 (3)
Ni-N(1)-C(1)	107.0 (6)	Ni-N(1)-C(8)	102.8 (5)
C(1)-N(1)-C(8)	120.4 (7)	Ni-N(1)-C(9)	102.8 (5)
C(1)-N(1)-C(9)	114.1 (7)	C(8)-N(1)-C(9)	107.7 (7)
Ni-N(2)-C(2)	104.4 (5)	Ni-N(2)-C(3)	103.2 (5)
C(2)-N(2)-C(3)	117.4 (7)	Ni-N(3)-C(4)	107.6 (5)
Ni-N(3)-C(5)	101.4 (5)	C(4)-N(3)-C(5)	120.5 (7)
Ni-N(4)-C(6)	106.9 (5)	Ni-N(4)-C(7)	101.7 (5)
C(6)-N(4)-C(7)	120.3 (7)	Ni-N(4)-C(10)	104.0 (5)
C(7)-N(4)-C(10)	114.5 (7)	C(7)-N(4)-C(10)	107.5 (8)
N(1)-C(1)-C(2)	108.6 (7)	N(2)-C(2)-C(1)	108.5 (8)
N(2)-C(3)-C(4)	110.9 (7)	N(3)-C(4)-C(3)	111.1 (7)
N(3)-C(5)-C(6)	107.4 (6)	N(4)-C(6)-C(5)	106.3 (6)
N(4)-C(7)-C(8)	105.6 (7)	N(1)-C(8)-C(7)	106.6 (7)
N(1)-C(9)-C(10)	105.4 (8)	N(4)-C(10)-C(9)	105.9 (7)

^aUnits of bond lengths are angstroms and of bond angles are degrees. For key to numbering scheme of atoms, see Figure 4.

Table V. Force Field Potential Function Constants for Complexes of Low-Spin and High-Spin Ni^{II} with Polyamine Ligands^a

	bond length force constants ^b			
	low-spin Ni^{II}		high-spin Ni^{II}	
	$r_{\text{Ni-N}}$	$K_{\text{Ni-N}}$	$r_{\text{Ni-N}}$	$K_{\text{Ni-N}}$
Ni-N	1.91 (1.89)	2.0 (1.5)	2.10	0.68
	bond angle force constants ^c			
	low-spin Ni^{II}		high-spin Ni^{II}	
	θ	K_θ	θ	K_θ
N-Ni-N (cis)	1.571	0.20 (0.3)	1.571	0.30
N-Ni-N (trans)	3.142	0.40 (0.3)	3.142	0.30
Ni-N-C	1.911	0.60 (0.2)	1.911	0.20
Ni-N-H	1.911	0.10	1.911	0.10
	nonbonded potential function constants ^d			
	a	b	c	
Ni--H	114	3.53	0.807	
Ni--C	689	3.64	1.990	

^aLow-spin Ni^{II} constants were developed in this work; those for high-spin Ni^{II} are from ref 24. Values in parentheses are those for the trial force field for low-spin Ni^{II} , where these were different from those in the final force field. Only parameters involving the nickel atom are reported here. For those for other atoms, ref 24 should be consulted.

^bUnits for the strain-free bond length, $r_{\text{Ni-N}}$, are Å and for the bond length deformation constant $K_{\text{Ni-N}}$ are $\text{mdyne}\cdot\text{Å}^{-1}$. ^cUnits for the bond angle deformation constants are the following: θ , radians; K_θ , $\text{mdyne}\cdot\text{Å}\cdot\text{radian}^{-1}$. ^dThese constants are from ref 30. The units are the following: a , $\text{erg}\cdot\text{molecule}^{-1}$; b , Å^{-1} ; c , $\text{erg}\cdot\text{Å}\cdot\text{molecule}^{-1}$.

subsequently by crystallography. It was found necessary to modify the trial force field to obtain overall improved structure prediction, but even so, the accuracy of structure prediction even with the trial force field was impressive. The trial parameters, together with the final refined set of force field parameters for the low-spin Ni^{II} ion, are seen in Table V, together with those used previously²⁴ for high-spin Ni^{II} . In Table VI are listed the more important bond angles and bond lengths as calculated by the refined force field and the values as actually observed in the crystal structures.

A technique for examining the response of the complex to change in metal ion size, which we have developed,^{10,25} involves keeping all the

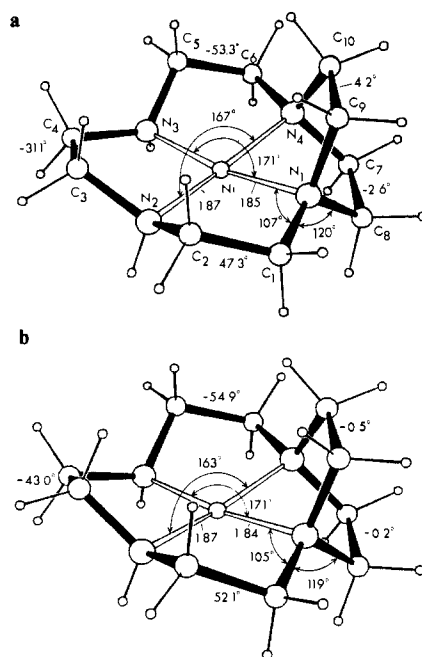


Figure 4. (a) ORTEP²³ drawing of the observed structure of the complex $[\text{Ni}((1,4\text{-C}_2)\text{-12-aneN}_4)]^{2+}$ showing the numbering scheme. Also shown are important bond angles, lengths, and torsion angles, which should be compared with those in Figure 4b. (b) The structure of $[\text{Ni}((1,4\text{-C}_2)\text{-12-aneN}_4)]^{2+}$ as predicted by molecular mechanics calculation prior to the crystallographic study reported in this paper, using the trial force field reported in Table V. The angles adjacent to bonds are the torsion angles about that bond and are actually those predicted using the refined force field in Table V.

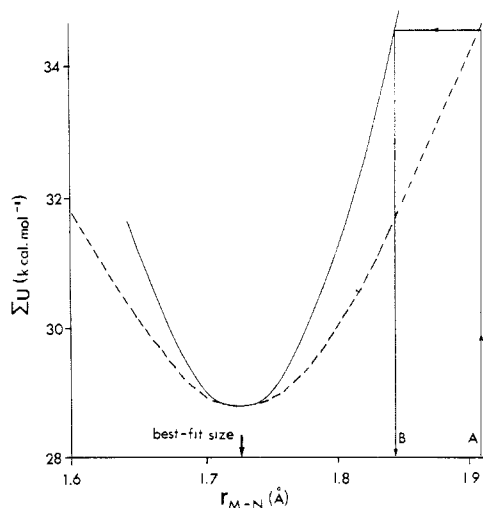


Figure 5. Total strain energy of the complex $[\text{Ni}((1,4\text{-C}_2)\text{-12-aneN}_4)]^{2+}$ as a function of the initial strain-free M-N bond length (---) and of the final energy-minimized M-N bond length (—), calculated as described in the text. The minimum in the curve indicates the best fit M-N length for fitting into the ligand. Point A is the strain-free bond length for low-spin Ni^{II} , and the arrows show how the diagram may be used to calculate the final energy-minimized Ni-N bond length of 1.85 Å.

parameters in the force field constant, except for the strain-free M-N length, which is varied systematically over the required range of M-N length. The minimum in the curve then corresponds to the best fit size for the metal ion coordinating to the ligand, while the shape of the curve indicates the sensitivity of the complex to change in metal ion size. We have carried out such a calculation for the complex $[\text{M}((1,4\text{-C}_2)\text{-12-aneN}_4)]^{2+}$ with parameters appropriate to low-spin Ni^{II} , varying the strain-free M-N bond length between 1.6 and 1.9 Å. The results of this calculation are presented graphically in Figure 5, where the strain energy

Table VI. More Important Bond Angles and Bond Lengths in Complexes of Low-Spin Nickel(II) with Polyamines, as Predicted by Molecular Mechanics Calculation and as Observed in Crystal Structures^a

struct param	[Ni(en) ₂] ²⁺ ^b		[Ni((1,4-C ₂)-12-aneN ₄)] ²⁺ ^c		[Ni(TMC)] ²⁺ ^d		[Ni(DMC)] ²⁺ ^e		[Ni(Me ₂ -13-aneN ₄)] ²⁺ ^f		[Ni(DACO) ₂] ²⁺ ^g	
	calcd	obsd	calcd	obsd	calcd	obsd	calcd	obsd	calcd	obsd	calcd	obsd
Ni-N	1.922	1.921	1.850	1.853	1.993	1.992	1.951	1.926	1.911	1.851	1.923	1.948
			1.852	1.872	1.968	1.978	1.951	1.940	1.886	1.895	1.923	1.953
			1.869	1.877	1.994	1.981	1.950	1.926	1.905	1.844	1.923	1.925
			1.851	1.865	1.968	1.980	1.952	1.940	1.905	1.877	1.923	1.897
N-Ni-N trans	180	180	171.2	170.8	169.9	169.0	179.8	180.0	169.2	175.2	179.6	172.0
			164.8	167.3	166.0	168.2	179.7	180.0	176.7	175.0	179.6	176.3
N-Ni-N cis	88.5	86.6	94.9	92.9	86.4	86.6	86.3	86.4	87.1	90.1	98.8	87.2
			91.5	93.6	77.3	80.5	94.8	94.3	93.5	93.6	89.6	85.3
Ni-N-C	106.6	109.2	91.8	92.6	94.9	95.0	93.9	93.6	93.2	94.8	81.2	93.1
			94.8	92.7	86.4	86.4	86.3	86.4	90.1	89.9	98.8	89.2
			104.4	106.8	108.4	108.6	118.3	119.8	106.3	107.5	115.9	114.9
			103.5	102.6	111.4	113.7	107.3	108.1	112.8	116.1	115.8	110.8
C-N-C			99.6	103.1	103.7	101.9	117.6	122.9	102.2	106.7	115.9	111.3
			99.8	101.4	114.3	114.2	108.6	109.4	111.5	106.7	115.8	112.2
			104.7	106.8	112.9	115.0	118.4	119.8	108.7	112.9	115.8	106.6
			117.4	120.5	105.5	107.4	107.5	110.1	111.8	106.0	113.6	113.4
N-C-C	106.0	105.4	116.0	114.1	105.3	106.8	110.6	112.5	114.7	117.1	113.6	113.5
			118.4	120.4	111.1	109.6	107.6	110.0	114.4	116.5	113.6	114.4
			114.9	114.5	105.5	107.6	110.4	112.5	113.0	110.1	113.6	113.7
			115.3	117.5	109.2	110.1						
C-C-C			107.2	108.9	107.4	107.8	105.8	107.0	105.9	100.8	118.6	112.6
			109.7	111.1	114.8	114.9	112.6	112.2	112.2	113.2	118.6	110.8
			105.1	106.2	106.8	107.4	113.2	111.3	104.6	107.9	118.6	111.7
			105.7	105.8	114.5	114.6	105.9	107.0	105.9	110.9	118.6	111.1
C-C-C					111.5	112.3	112.1	113.5	113.0	113.3	118.7	117.4

^a Bond lengths are in angstroms, and angles, in degrees. For key to abbreviations for ligands, see Figure 1. The force field parameters for the molecular mechanics calculations are those listed in Table V or referenced therein. ^b Observed structural parameters from ref 8. ^c Observed structural parameters, this work. ^d Observed structural parameters, ref 12. ^e Observed structural parameters, ref 13. ^f Structure from ref 15. The *R* factor reported for this structure is 0.14, so that the poorer agreement between calculated and observed values is not significant. ^g From ref 14. Again, the *R* factor for this structure is very high, accounting for the poorer level of agreement between calculated and observed parameters.

of the complex is plotted as a function of both the strain-free M-N bond length and the final energy-minimized M-N length indicated by the program.

Results and Discussion

Formation Constant Studies. The protonation constants for (1,4-C₂)-12-aneN₄ are seen in Table I, along with those for its nonbridged analogue, 12-aneN₄. The protonation constants for (1,4-C₂)-12-aneN are remarkable in that they show a smooth decrease in size as the number of protons on the ligand increases. This is in marked contrast to other tetraaza macrocycles, where there is a large drop in p*K* between p*K*₂ and p*K*₃. This has been interpreted²⁶ in terms of the nitrogens having to change from an endo conformation, where the coordinated protons lie in the cavity of the macrocycle, to an exo conformation, where the nitrogens are oriented outward and the protons are on the outside of the ligand. The protonation constants for (1,4-C₂)-12-aneN₄ are more like those of an open-chain ligand, which suggests that the ligand may have an exo conformation even before any protons are added.

The formation constants in Table I indicate very considerable stability for the complexes of (1,4-C₂)-12-aneN₄. This is particularly so in comparison with those of the ligand BAE-PIP (*N,N'*-bis(2-aminoethyl)piperazine), the open-chain polyamine analogue of (1,4-C₂)-12-aneN₄. The size of the macrocyclic effect, log *K* (MAC), for Cu^{II} and Ni^{II} at 9.6 log units for the (1,4-C₂)-12-aneN₄ complexes relative to those of BAE-PIP, is by far the largest for any macrocyclic system that we could find. Thus, in tetraaza macrocycles, log *K* (MAC) is typically only 3–6 orders

of magnitude. An important aspect of the log *K* (MAC) values in Table I is the way that they vary with metal ion size. For 12-aneN₄, the log *K* (MAC) values tend to be smaller with small metal ions and larger with large metal ions. This indicates that the small cavity in 12-aneN₄ is not able to exert any selectivity in favor of small metal ions, in line with the ability of the 12-aneN₄ complexes of large metal ions to adopt the *trans*-I conformer and be coordinated lying well out of the plane of the nitrogen donors of the ligand. On the other hand, log *K* (MAC) for (1,4-C₂)-12-aneN₄ is very large for small metal ions but falls off very rapidly as metal ion size increases, indicating that the ligand is able to discriminate against large metal ions. If we compare the stabilities of the (1,4-C₂)-12-aneN₄ and 12-aneN₄ complexes, we see that the difference in the stability of the complexes, Δlog *K*, also decreases rapidly with increasing metal ion size, supporting once again the idea that the more rigid cavity of (1,4-C₂)-12-aneN₄ has led to greater ability to discriminate against large metal ions. One might speculate here on the very large value of log *K* (MAC) for (1,4-C₂)-12-aneN₄ of over 9 orders of magnitude with Ni^{II} and Cu^{II}. Several suggestions can be made. One is that the low-energy conformation of cyclohexane-type rings is normally the chair form, and there are no constraints on the piperazine ring present in BAE-PIP from assuming the preferred chair form in the free ligand. However, on coordination, the piperazine part of the ligand is obliged to switch to the energetically less favorable boat form. In contrast, even in the free ligand (1,4-C₂)-12-aneN₄, it is not possible for the piperazine ring present to assume the chair form, and this unfavorable contribution to complex formation would therefore not be present. Another suggestion relates to the way in which the piperazine ring in complexes of BAE-PIP acts rather like a spring to pull the amine groups on the aminoethyl "arms" of the ligand away from the coordinated metal ion, thereby destabilizing the complex. Tying the terminal amines of BAE-PIP together with a bridging ethylene group to give (1,4-C₂)-12-aneN₄ may help to overcome such sources of destabilization. Another possible contribution may come from the very small cavity of (1,4-C₂)-12-aneN₄, which would promote desolvation of the nitrogens along the lines suggested by Hinz and Margerum³¹ to

(26) Micheloni, M.; Sabatini, A.; Paoletti, P. *J. Chem. Soc., Perkin Trans. 2* **1978**, 828–830.

(27) Hancock, R. D.; Evers, A.; Ngwenya, M. P., to be submitted for publication.

(28) Shannon, R. D. *Acta Crystallogr., Sect. A: Cryst. Phys., Diffraction, Gen. Crystallogr.* **1976**, *32*, 751–767.

(29) Martell, A. E.; Smith, R. M. *Critical Stability Constants*; Plenum: New York, 1974–1982; Vols. 1–5.

(30) Boeyens, J. C. A.; Cotton, F. A.; Han, S. *Inorg. Chem.* **1985**, *24*, 1750–1753.

account for the large enthalpy contribution to the macrocyclic effect.

Structure of $[\text{Ni}((1,4\text{-C}_2)\text{-}12\text{-aneN}_4)](\text{ClO}_4)_2$. The complex cation is seen in stereoview in Figure 3. Important bond lengths and angles are seen in Table IV. The Ni–N bond lengths, with a mean value of 1.867 (4) Å, are very short compared with the Ni–N bond lengths⁸ of 1.92 (1) Å in $[\text{Ni}(\text{en})_2]^{2+}$. This supports the idea¹¹ that there might be compression in the Ni–N bonds of $[\text{Ni}((1,4\text{-C}_2)\text{-}12\text{-aneN}_4)]^{2+}$ causing the very high LF strength in the complex. The structure also shows that the Ni is forced some 0.2 Å out of the mean plane formed by the four nitrogen donor atoms, which is unusual for a complex of low-spin Ni^{II}. This forcing of the metal ion out of the plane of the donor atoms is a further sign that the metal ion is under compressive forces. Another feature of interest in the structure is the piperazine-type ring, which has an almost exact boat conformation, as well as C–N–C angles, which are in many cases much larger than the strain-free value of 109.5°, suggesting that they are being opened out by return pressure from the compressed Ni ion. However, to analyze these features more fully, it is necessary to consider the MM calculations.

Molecular Mechanics Calculations on Polyamine Complexes of Low-Spin Ni^{II}. In Table V are seen the force field parameters developed here for polyamine complexes of low-spin Ni^{II}. It is seen that, in line with the greater covalence expected in the M–L bonds of low-spin Ni^{II}, the Ni–N bond length deformation constant and the N–Ni–N and Ni–N–C bond angle deformation constants are very much larger for low-spin Ni^{II} than for high-spin Ni^{II}. The strain-free Ni–N bond length in low-spin Ni^{II} is 1.91 Å. The very short value for this constant of 1.83 Å reported¹² by Hambley is unable to reproduce structures of complexes of low-spin Ni^{II} other than that of $[\text{Ni}(\text{TMC})]^{2+}$ analyzed by Hambley. For example, use of the full set of force field parameters reported by Hambley¹² to predict the structure of $[\text{Ni}(\text{en})_2]^{2+}$ suggests a Ni–N bond length of 1.86 Å, which is considerably shorter than the observed⁸ value of 1.92 Å. We thus recommend the force field parameters obtained in this work, and reported in Table V, for MM calculations on complexes of low-spin Ni^{II} rather than those reported by Hambley.¹²

Inspection of Table VI shows that the accuracy of prediction of the structures of the complexes $[\text{Ni}(\text{en})_2]^{2+}$, $[\text{Ni}((1,4\text{-C}_2)\text{-}12\text{-aneN}_4)]^{2+}$, $[\text{Ni}(\text{TMC})]^{2+}$, and $[\text{Ni}(\text{DMC})]^{2+}$ is highly satisfactory. In particular, the use of the strain-free Ni–N bond length of 1.91 Å permits the satisfactory prediction by MM calculation of the observed Ni–N bond lengths over a range of 1.84–1.99 Å. One can thus conclude that the strain-free bond length in complexes of low-spin Ni^{II} with polyamine ligands is 1.91 Å, only slightly shorter than observed⁸ in the low-strain complex $[\text{Ni}(\text{en})_2]^{2+}$.

Both the MM calculations and the crystal structure of $[\text{Ni}((1,4\text{-C}_2)\text{-}12\text{-aneN}_4)]^{2+}$ suggest that in this case the Ni–N bond length is being compressed by approximately 0.05 Å. However, the structure and MM calculations allow us to identify other structural features besides M–N bond length that should be considered when postulating compression of a metal ion. The ligand is not infinitely rigid and should also show distortion due to return pressure from the compressed metal ion. In particular, the compression of the metal ion should cause considerable pressure on the nitrogen (or other) donor atoms, resulting in a bending of the C–N–C angle to values larger than the ideal value of 109.5°. In accord with this, it is seen that in the structures of $[\text{Ni}(\text{TMC})]^{2+}$ and $[\text{Ni}(\text{DMC})]^{2+}$, where there is in fact Ni–N bond length stretching, the C–N–C angles are all less than or close to 109.5°. In $[\text{Ni}((1,4\text{-C}_2)\text{-}12\text{-aneN}_4)]^{2+}$, where we have proposed compression of the nickel, we see C–N–C angles in the vicinity of 120°. One might suppose that the somewhat larger C–N–C angles in $[\text{Ni}(\text{Me}_2\text{-}13\text{-aneN}_4)]^{2+}$ are symptomatic of compression of the metal ion. However, as seen in Table VI, the MM calculations reproduce these larger C–N–C angles, even though the same calculations show little compression of the Ni–N bond length, this being less than 0.01 Å. The larger C–N–C angles in $[\text{Ni}(\text{Me}_2\text{-}13\text{-aneN}_4)]^{2+}$ are thus probably a feature of ligand geometry.

This can be demonstrated by repeating the MM calculations with very short Ni–N bond lengths of 1.7 Å. Here, there is in $[\text{Ni}(\text{Me}_2\text{-}13\text{-aneN}_4)]^{2+}$ now very clearly considerable Ni–N bond stretching, but still the C–N–C angles remain at several degrees larger than the ideal value of 109.5°. On the other hand, if the strain-free Ni–N bond length used in the MM calculation on $[\text{Ni}((1,4\text{-C}_2)\text{-}12\text{-aneN}_4)]^{2+}$ is shortened to 1.7 Å, the C–N–C angles come down considerably in size to fall in the range 110–114°, supporting the idea that they are forced out to values close to 120° in the complex by force exerted on the nitrogen donor atom by the compressed Ni–N bond. Another symptom of metal ion compression in crystal structures of complexes of metal ions with square-planar coordination geometry is the fact of the metal ion being extruded from the plane of the donor atoms in an attempt to lessen compressive forces. Thus, as reproduced by the MM calculations, the nickel atom lies some 0.2 Å out of the plane of the four donor atoms in the complex $[\text{Ni}((1,4\text{-C}_2)\text{-}12\text{-aneN}_4)]^{2+}$ but lies more or less in the plane of the donor atoms in $[\text{Ni}(\text{Me}_2\text{-}13\text{-aneN}_4)]^{2+}$. The rather short Ni–N bond lengths reported in the structure¹⁵ or $[\text{Ni}(\text{Me}_2\text{-}13\text{-aneN}_4)]^{2+}$ are suggestive of compression, but the MM calculations in Table VI do not support this. The high *R* factor associated with the structure¹⁵ of $[\text{Ni}(\text{Me}_2\text{-}13\text{-aneN}_4)]^{2+}$ leads us to prefer the indications of the MM calculations at this stage until other evidence becomes available. Work in progress³² has in fact supported completely the predicted Ni–N bond lengths for Ni(II) complexes of 13-aneN₄-type ligands.

We have previously^{10,25} reported a method whereby the best fit size of a metal ion into a particular ligand may be determined by scanning the total strain energy of a complex as a function of metal ion size. In Figure 5 is shown the plot of the strain energy of the $[\text{M}((1,4\text{-C}_2)\text{-}12\text{-aneN}_4)]^{2+}$ ion as a function of both the strain-free M–N bond length, and the final energy-minimized M–N bond length.

When the calculation was carried out, all the parameters used were kept constant at those for low-spin Ni^{II}, except that the value of the strain-free Ni–N bond length was varied in steps of 0.05 Å from 1.60 to 1.90 Å. The minimum in the curve shown in Figure 5 thus corresponds to the best fit size for a square-planar metal ion coordinating to the ligand (1,4-C₂)-12-aneN₄. It is seen that the minimum occurs at a M–N bond length of 1.73 Å, this being then the best fit size of M–N bond length for fitting into the macrocycle. It is thus apparent that low-spin Ni^{II} with a M–N strain-free length of 1.91 Å is considerably too large to fit into (1,4-C₂)-12-aneN₄. It is thus remarkable that the complex of low-spin Ni^{II} with (1,4-C₂)-12-aneN₄ is not significantly less stable than that with 12-aneN₄, which in its *trans*-I or possibly *trans*-III conformers, provides a much better fit for low-spin Ni^{II}.⁷

Figure 5 shows how a metal ion such as low-spin Ni^{II} will have its strain-free bond length of 1.91 Å (point A) compressed down to a value of about 1.85 Å (point B). Diagrams such as Figure 5 are useful in allowing one to read off changes in M–L bond length in this way. As stated above, the amount of compression of the Ni–N bond in the complex $[\text{Ni}((1,4\text{-C}_2)\text{-}12\text{-aneN}_4)]^{2+}$ appears to be approximately 0.05 Å (the MM calculations suggest 0.06 Å, while the crystal structures suggest 0.04 Å). It is almost certain that this compression must contribute substantially to the high in-plane LF observed¹¹ in $[\text{Ni}((1,4\text{-C}_2)\text{-}12\text{-aneN}_4)]^{2+}$. It is an open question, however, whether compression of the Ni–N bond by 0.05 Å accounts for the whole of the very substantial increase in LF strength. One notes that LF strength increases strongly along the series $[\text{Ni}(\text{NH}_3)_6]^{2+}$, $[\text{Ni}(\text{en})_3]^{2+}$, and $[\text{Ni}(\text{9-aneN}_3)_2]^{2+}$, where there is crystallographically no evidence of compression. This effect has been attributed^{6,10} to the increasing basicity along the series $\text{NH}_3 < \text{RNH}_2 < \text{R}_2\text{NH} < \text{R}_3\text{N}$. We thus note that 12-aneN₄ has four secondary nitrogens, whereas (1,4-C₂)-12-aneN₄ has two secondary and two tertiary nitrogens. We thus

(32) Billo has indicated a Ni–N bond length of 1.895 Å in $[\text{Ni}(\text{13-aneN}_4)][\text{Zn}(\text{Cl})_4]$, in remarkable agreement with the predicted mean Ni–N length of 1.902 Å, supporting the idea that there is at best only a small amount of Ni–N bond length compression in the $[\text{Ni}(\text{13-aneN}_4)]^{2+}$ cation: Billo, E. J., personal communication.

(31) Hinz, D.; Margerum, D. W. *Inorg. Chem.* 1974, 13, 2941.

suggest that a substantial part of the higher LF strength in $[\text{Ni}((1,4\text{-C}_2)\text{-}12\text{-aneN}_4)]^{2+}$ will come from the presence of tertiary nitrogens on the ligand. One might ask why one does not normally see very high LF strengths in other situations where tertiary nitrogens are present, such as $[\text{Ni}(\text{TMC})]^{2+}$, with its *N*-methyl groups. The answer is apparent in Table VI. Normally, adding alkyl groups to a secondary nitrogen to create a tertiary nitrogen leads to a sterically crowded situation, and the M–N bonds are accordingly stretched to relieve the steric crowding. This is seen in Table VI, where the MM calculations show that the Ni–N bond length in $[\text{Ni}(\text{TMC})]^{2+}$ has been stretched by some 0.07 Å due to van der Waals repulsion between the *N*-methyl groups. Only a ligand such as $(1,4\text{-C}_2)\text{-}12\text{-aneN}_4$ is of a suitable geometry that tertiary nitrogens can be present without leading to a high degree of steric strain and resulting M–N bond length stretching, allowing the higher intrinsic LF strength of the tertiary nitrogen to be observed.

In the introduction it was suggested that the *trans*-III conformers might be able to compress too large metal ions but that this was avoided by means of the complex adopting other conformers such as the *trans*-I (Figure 2). It is of interest here to compare the metal ion compressing ability of the *trans*-III conformer of 12-aneN_4 with that of $(1,4\text{-C}_2)\text{-}12\text{-aneN}_4$ by means of MM calculation. Because of its high strain energy,⁷ it seems probable that no complex of 12-aneN_4 will ever be observed to have the *trans*-III conformation, but *trans*-III $[\text{Ni}(12\text{-aneN}_4)]^{2+}$ can be generated by MM calculation. It is found that the Ni–N bond length in this complex is predicted to be 1.86 Å, very close to the mean Ni–N bond length predicted for $[\text{Ni}((1,4\text{-C}_2)\text{-}12\text{-aneN}_4)]^{2+}$. This makes the surprising suggestion that the extra bridge on $(1,4\text{-C}_2)\text{-}12\text{-aneN}_4$ does not add much to the compressive ability of the ligand relative to the *trans*-III conformer of 12-aneN_4 but mainly serves to prevent the ligand from folding to adopt conformers like the *trans*-I or *cis*-V, which are more easily able to accommodate large metal ions.

Other Doubly Bridged Ligands. We have embarked on a program of synthesizing other doubly bridged ligands and have already synthesized some of those shown in Figure 1, such as $(1,4\text{-C}_2)\text{-}15\text{-aneN}_4$, $(1,4\text{-C}_2)\text{-}15\text{-aneN}_5$, and $(\text{C}_2)_2\text{-}18\text{-anN}_2\text{O}_4$. The piperazine part of the molecule appears to act like a spring and holds the cavity in the ligand open. Nonbridged 15-aneN_5 is able to coordinate too-small octahedral metal ions such as high-spin

Ni^{II} or Zn^{II} very satisfactorily, because the ligand can fold and coordinate to the metal ion; i.e., the nonrigid cavity collapses. However, the rigid cavity of a ligand such as $(1,4\text{-C}_2)\text{-}15\text{-aneN}_5$ cannot collapse and coordinate small metal ions. We thus find that it coordinates very strongly to large metal ions such as Cd^{II} but suffers a 13 order of magnitude drop in formation constant in passing from the Cu^{II} complex of 15-aneN_4 to $(1,4\text{-C}_2)\text{-}15\text{-aneN}_5$. The doubly bridged ligand $(\text{C}_2)_2\text{-}18\text{-aneN}_4\text{O}_2$ is remarkable in that it coordinates only the large metal ion Pb^{II} , showing size-match selectivity greatly superior to that shown by any unbridged ligand. We are also interested in investigating double bridges of other sizes. Molecular mechanics calculations show that, whereas the double five-membered chelate ring formed by coordination to piperazine will have lowest strain energy with very large metal ions, the double chelate ring formed by DACO will prefer very small metal ions and the homopiperazine-type of ring will prefer medium-sized metal ions. Inspection of Table I shows that, in support of the MM calculations, the drop in stability on going from trien complexes to those of BAE-PIP is greatest for small metal ions and least for large ones. This is in line with the idea that large metal ions will coordinate best to a piperazine ring in the absence of other steric constraints such as the macrocyclic ring of small size present in $(1,4\text{-C}_2)\text{-}12\text{-aneN}_4$. On the other hand, we have found that DACO does not coordinate to the large metal ions Pb^{II} , Cd^{II} , or even the medium-sized Zn^{II} but only to the small metal ions Cu^{II} and low-spin Ni^{II} , while BAE-DACO does not coordinate to Cd^{II} or Pb^{II} . We thus are examining the coordinating properties of macrocycles, which contain double linkages of other sizes, such as $(10,13\text{-C}_2)\text{-}13\text{-aneN}_4$ and $(4,8\text{-C}_3)\text{-}14\text{-aneN}_4$ shown in Figure 1.

Acknowledgment. We thank the Council Research Grants Committee of the University of the Witwatersrand and the Foundation for Research Development, for generous financial support for this work.

Registry No. $[\text{Ni}((1,4\text{-C}_2)\text{-}12\text{-aneN}_4)](\text{ClO}_4)_2$, 82404-79-3.

Supplementary Material Available: Listings of anisotropic temperature factors for $[\text{Ni}((1,4\text{-C}_2)\text{-}12\text{-aneN}_4)](\text{ClO}_4)_2$ and fractional coordinates for hydrogen atoms (3 pages); listing of observed and calculated structure factors (9 pages). Ordering information is given on any current masthead page.